

Advances of MOEMS-based External Cavity QCLs

M. Haertelt^{a,*}, S. Hugger^a, L. Butschek^a, C. Schilling^a, A. Merten^b, M. Schwarzenberg^b, A. Dreyhaupt^b, J. Grahmann^b, M. Rattunde^a, R. Ostendorf^a

^aFraunhofer Institute for Applied Solid State Physics, Tullastrasse 72, 79108 Freiburg, Germany;

^bFraunhofer Institute for Photonic Microsystems, Maria-Reiche-Strasse 2, 01109 Dresden, Germany

ABSTRACT

The combination of broadly tunable quantum cascade laser chips in an external cavity (EC-QCL) with a micro- electro-mechanical system (MEMS) scanner with integrated diffraction grating as wavelength-selective element allows for the development of extremely compact and robust spectroscopy systems. Resonant MOEMS grating scanners enable spectral tuning rates of hundreds of wavenumbers per millisecond and consequently broad-band spectroscopy with millisecond temporal resolution. Also non-resonant (quasistatic) MOEMS grating scanners are possible, providing scan rates of tens of Hz as well as static setting of arbitrary wavelengths, as common for mechanically driven EC lasers, while keeping the small MOEMS footprint, ruggedness, and low power consumption. Here, we give a progress report on the latest developments on MOEMS-based EC-QCLs made by Fraunhofer IAF and IPMS. We will highlight two of our latest developments: A non-resonant MOEMS EC-QCL version that allows arbitrary scan frequencies up to few ten Hertz, as well as static operation. Furthermore, we present the application of a resonantly driven cw-MOEMS-EC-QCL with cavity-length control to enable fast high-resolution spectroscopy over a spectral range of $>100\text{ cm}^{-1}$, offering new possibilities for spectroscopy on complex gas mixtures.

Keywords: quantum cascade lasers, micro-electro-mechanical system scanners, high resolution spectroscopy, gas spectroscopy, real-time spectroscopy

1. INTRODUCTION

Quantum cascade lasers (QCL) are the ideal laser sources for vibrational spectroscopy as they combine wide spectral tunability in the fingerprint region of most molecules with small footprint and low power consumption. In contrast to incoherent sources, such as glow bars, tunable quantum cascade lasers provide exceptional brilliance. Compact and rugged devices based on such laser sources bear great potential as an enabling technology to transfer mid-IR spectroscopy from the lab to the field use. To exploit the full tuning range of quantum cascade lasers, which for heterocascading QCL structures can exceed more than 500 wavenumbers,¹ most commonly external cavities with a wavelength selective grating are utilized. The tuning speed of such a device is given by the mechanics driving the grating, which is most commonly a piezo or stepper motor driven stage. However, also galvo mirrors² can be employed. Alternatively, micro-opto-electro-mechanical system (MEMS) scanners with integrated diffraction grating (micro-opto-electro-mechanical-systems - MOEMS) allow further miniaturization and increased the tuning speeds.^{3,4} Up to now, resonantly driven MOEMS scanners in an external cavity with the QCL chip have been realized. These allow measurement speeds of up to 1000 spectra per second and are the ideal light source for handheld devices.⁵⁻⁷

Other applications may not require such continuous and high tuning speeds, which can even be cumbersome as they are more demanding for the data acquisition and require fast single pulse detection. For detectors with slower time constants, such as for pyrodetectors, but also in case the time constants for the application are too long, as for photothermal or photoacoustic spectroscopy, slower tuning speeds or even addressing only single selected wavelength is desirable. In section 2, we will present a quasi-static MOEMS-EC-QCL, which allows to tune the laser source to discrete wavelength, as common for conventional EC-QCLs, but also allows for almost arbitrary trajectory movements, with repetition rates up to 50 Hz. The quasi-static MOEMS-EC-QCL module is matchbox-sized, illustrating the compactness achievable with MOEMS scanners.

*marko.haertelt@iaf.fraunhofer.de

Another topic that we address is the spectral resolution of the resonantly driven MOEMS-EC-QCL. In the case of pulsed lasers, the spectral resolution is determined by the thermal chirp during the laser pulse, which limits the spectral resolution to about 1-2 wavenumbers for typical pulse length of 100-200ns. In the case of cw-lasers, the spectral resolution is typically on the order of milli-wavenumbers, but in addition also limited by the mode structure. The commonly employed Littrow-resonator geometry illustrated in figure 1 allows for very compact laser modules, however, the facets of the laser chip form a Fabry-Pérot resonator, the internal resonator. The laser facet on the resonator side, on the other hand, form with the grating the external resonator. While tuning the wavelength the emission wavelength is determined by the competition of the two and the feedback provided by the grating, which acts as an additional spectral filter. In a typically EC-QCL the free spectral range of the two resonators are not matched to each other, which causes a hardly predictable behavior of the mode structure during a wavelength tuning. EC-QCLs using conventional rotation stages for the grating angle in combination with a precise external cavity length-control using an additional linear stage and laser current scan changing the length of the chip resonator, have allowed for locally mode-hop free tuning over a couple of wavenumbers by employing a careful longitudinal mode tracking.⁸ The mode hop free tuning range was governed here by the range of laser current available for single mode scan and limited to a few cm^{-1} . Continuous mode-hop free tuning over more than 100 cm^{-1} has been achieved by a more refined mechanical engineering.⁹ We transfer the concepts from Ref [8] to the resonant MOEMS-EC-QCL and demonstrate in section 3 high resolution spectroscopy with such a laser source over the whole tuning range of the QCL.

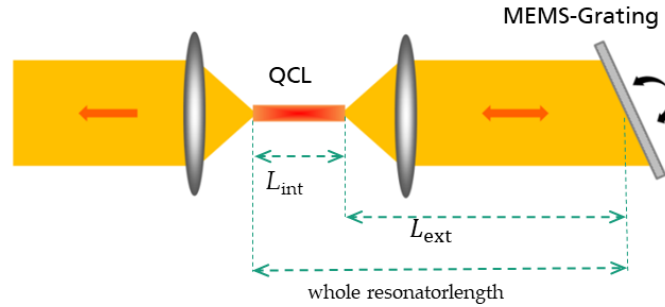


Figure 1. Schematics of a (MOEMS) EC-QCL setup in Littrow configuration.

2. QUASI-STATIC MOEMS EC-QCL

The MOEMS grating scanner presented here and shown as a schematic in Fig. 2a is a micromirror made from $75 \mu\text{m}$ thick crystalline silicon with a torsional axis. A grating is etched into the micromirror with the grating orientation parallel to the torsional axis. The movable driving electrodes of the electrostatic comb drives are installed between the scanner plate and the torsional anchors. Opposite of them are the fixed driving electrodes, highlighted in red and blue in the schematics. The micromirror and the movable driving electrodes are kept on ground potential. A deflection is typically achieved by applying a voltage between the two. For a resonant MOEMS scanner,⁴ fixed and movable driving electrodes are in the same plane when in their equilibrium position. To operate such a resonant scanner, a rectangular voltage is applied to the electrodes. After a settling phase, the MOEMS scanner follows an almost perfectly sinusoidal trajectory, which amplitude is governed by the applied voltage, frequency, and the damping. The oscillation frequency can be varied close to the resonance frequency by a few hertz. A static deflection cannot be achieved in such a configuration. To achieve a static deflection, a staggered vertical comb drive is integrated, i.e. the static and movable driving electrodes are shifted out-of-plane to allow for the application of a static moment.¹⁰ To achieve such an offset, a wafer level bonding process is used, in which an additional lid wafer is added to the device. This lid wafer, pushes the static driving electrodes out of their plane by $75 \mu\text{m}$.¹⁰ After finishing the bonding process, the outer combs are fixed by the lid wafer and form the fixed driving electrodes. Such static controllable MOEMS scanner allow arbitrary torsional movements well below their mechanical resonance frequency, with typical repetition rates from 0.1 to 50 Hz.¹²

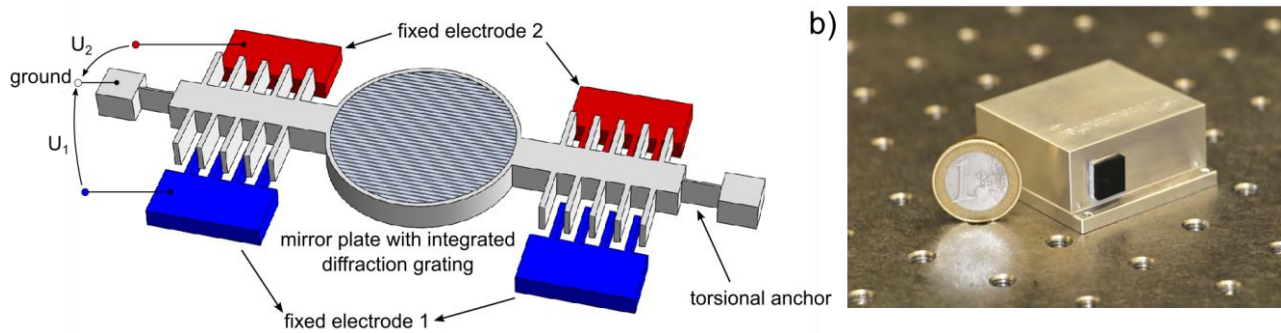


Figure 2. a) Schematics of the quasi-static MOEMS micromirror with integrated diffraction grating. The static electrodes of the staggered vertical comb drives are highlighted in red and blue. The (static) potentials are applied to those.¹¹ b) Picture of the integrated quasi-static MOEMS EC-QCL module.

Piezo-resistive sensors from polycrystalline silicon and wired in a Wheatstone half-bridge are integrated in the device symmetrically to the anchor points of the torsional suspension, which allows to measure the mechanical stress. A torsional movement is measurable as a bridge voltage with high signal-to-noise ratio.¹⁰ For quasi static devices the integrated sensor allows to realize a closed-loop feedback control, which enables precise control for linear or complex trajectories.¹²

The fabrication of the grating into the scanner plate was integrated in the MEMS manufacturing process. Details of the process have been described elsewhere.⁴ For the device presented here, a trapezoidal grating with 240 l/mm and a maximum efficiency at 4.3 μm for TM-polarization was integrated. The MOEMS scanner is mounted on a 2 mm thick Si₃N₄-ceramic. Electrical connections are made by using a flex cable. To allow for easier installation of the whole device in the desired Littrow-configuration, the MOEMS is put on an aluminium wedge.

The quasistatic MOEMS is controlled by an electronics board based on an ARM Cortex microcontroller. It is capable in generating the high voltage signal for both electrostatic combs, to read out the current amplitude from the position sensor, and has a closed loop controller implemented.

The electromechanical properties of the MOEMS, such as the static deflection curve, the resonance frequency, the damping, as well as the calibration of position sensor have been characterised for the isolated module. Static deflection curves have been measured simultaneously with the voltages on the position sensor, which allowed to calibrate the sensor. The results from the characterisation are used in the generation of voltage trajectories for a desired deflection curve, such as sawtooth or triangular curve, and the determination of the regulation parameter. To avoid a stimulation of the resonance mode, jerk-limited trajectories are calculated. The closed-loop control allows furthermore to suppress excitation of the resonance mode.

The quasistatic MOEMS grating was integrated in a module (see Figure 2b) with the QCL chip, the laser driver and parts of the MOEMS sensor electronics. All components are built up on a ceramic baseplate. This module measures only 6 x 4.5 x 2 cm³, illustrating the extremely small footprint achievable for QCL laser modules based on MOEMS gratings. The grating is pre-aligned in the module, such that the default grating position is matched with the center wavelength of the QCL chip. The length of the external resonator L_{ext} (see figure 1) measures only 7-8 mm.

The wavelength reproducibility and accuracy was tested in pulsed mode by measuring the emission wavelength using an FTIR spectrometer. The EC-QCL was tuned statically with the help of the MOEMS grating in steps of 0.1° from -1° to 0.9°. Every 0.2°, the measurement was repeated 3 times. Between each repetition, the deflection was changed to 1.0° to test the reproducibility. The results are shown in Fig. 3 a-e. The measurements show narrow emission lines common for

such pulsed lasers. Figures 3b to e reveal that the quasistatic MOEMS can move to the desired wavelength very reproducibly, as hardly any differences between 3 repeated measurements at the same deflection angle are observed.

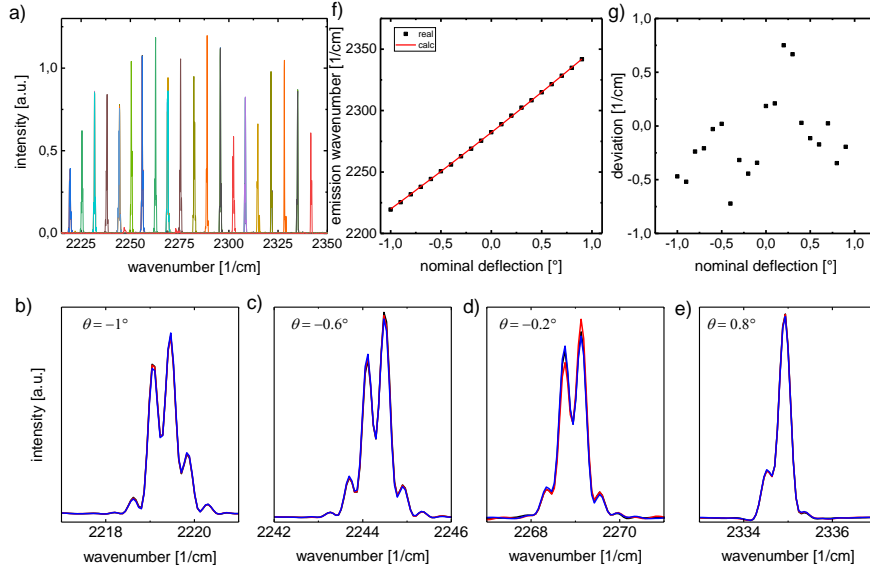


Figure 3. a) Linewidth and reproducibility measurement using an FTIR spectrometer for different static deflection angular settings between -1° and 0.9° in steps of 0.1° . Every 0.2° the measurements have been repeated 3 times, each time the MOEMS was reset to 1° before the measurement. b to e show some of the emission lines in more detail for selected deflection angles θ . Differences between the 3 scans can hardly be resolved, which illustrate the good wavelength reproducibility. f) Plot of the wavelength accuracy. g) Plot of the wavelength deviation.

In Figure 3f, we plot the emission wavelength determined by the FTIR spectrometer as a function of the nominal (or set) deflection angle θ . The emission wavelength is calculated via

$$\lambda = 2 \cdot g \cdot \sin(\theta_0 + \theta)$$

From the measured wavelength at $\theta=0^\circ$ the central deflection angle θ_0 was determined as $\theta_0=31.72^\circ$. The difference between emission wavelength and expected wavelength is plotted in Fig. 3f. The maximum difference between the two is 0.75 cm^{-1} , which is very good considering that the Fabry-Perot mode spacing of the QCL chip is $\sim 0.4 \text{ cm}^{-1}$. Some of the variation might be due to strong CO_2 absorptions in this wavelength range, which causes difficulties in determining the centre of the emission wavelength. However, because of the very good wavelength reproducibility between scans the deviations can be corrected for in an additional calibration process.

The intensity spectrum of the QCL for a scanning quasistatic MOEMS grating, following a 10 Hz triangular trajectory is shown in Fig. 4 for 30 consecutive scans. The QCL chip was operated in pulsed mode (400 kHz repetition rate and 100 ns pulse duration). The measurement of the intensity was done by using a thermoelectrically cooled HgCdTe-detector and a DAQ system able to record single pulses, i.e. each sampling point corresponds to a laser pulse. The data is processed by using a rolling average over 20 points. A trigger is provided by the MOEMS electronics for synchronization. Above 2300 wavenumbers strong absorptions due to CO_2 in the atmosphere are visible. In the same figure we also plot the normalized standard deviation calculated from the 30 scans, illustrating the good wavelength reproducibility of the laser source. In the range of the CO_2 absorption region, the noise is strongly increased.

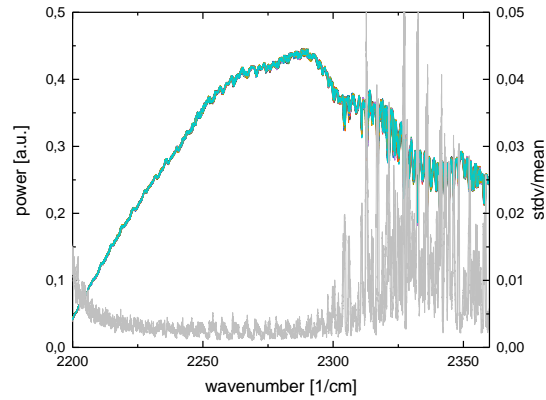


Figure 4. Intensity plots for 30 periods in pulsed mode for a scanning MOEMS grating following a triangular trajectory with 10 Hz scan frequency. The data was smoothed by using a 20 points running average. For wavelength larger than 2300 cm^{-1} strong CO_2 absorptions are observed, which also cause a dramatic increase in noise, which is plotted in the same graph.

A fast characterisation of the spectral accuracy over the whole spectral tuning range can be done by using the interference fringes of a thin GaAs plate, as in a transmission measurement periodic etalon structures evolve. Such an approach is especially useful under dynamic conditions, as the change in the emission wavelength is too fast to be resolved with an FTIR spectrometer. In Fig. 5 we show the results of the measurement in comparison to a simulated transmission assuming infinitely narrow linewidth of the laser emission. A good agreement in terms of position of the maxima is found between simulation and experiment. The reduced modulation depth in the measured curve is due to the finite linewidth of the laser. For closed-loop operation, the measurement results show a small shift of up to 1 cm^{-1} between forward and backwards movement of the 10 Hz triangular trajectory. This discrepancy is within the wavelength accuracy observed before. Due to the proven high repeatability of the MOEMS scanner, these wavelength offsets can be corrected for already during the characterisation of the device.

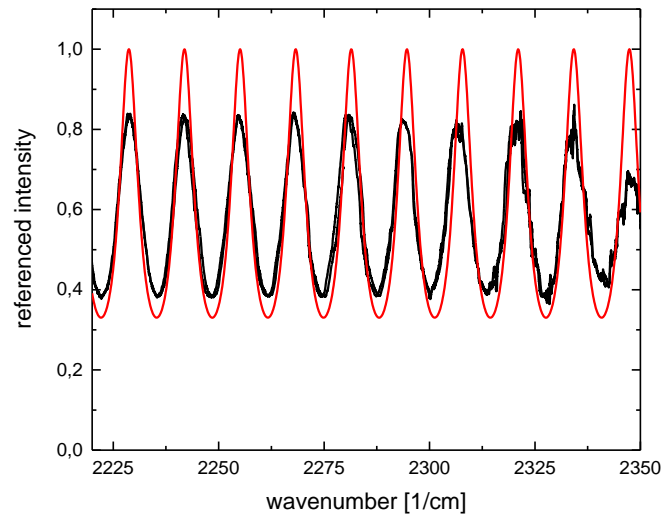


Figure 5. The transmission measurement through a GaAs wafer shows a pronounced etalon effect. In black are the results from the measurement with the laser operated in pulsed mode and the MOEMS grating running at a 10 Hz repetition rate for forward and backward motion. For the simulation we assume a refractive index of $n=3.2$ and a thickness of $114\text{ }\mu\text{m}$. The assumed linewidth is zero.

3. MOEMS-EC-QCL BASED HIGH RESOLUTION SPECTROSCOPY

The resonant MOEMS EC-QCL described in Refs. [3-7] operating at a resonance frequency of roughly 1 kHz allows real time spectroscopy with spectral scan speeds of almost 1000 spectra per second. The spectral resolution however is limited. Mode-hop free tuning is not directly feasible with this device, but the approach described in Ref. [8] can be implemented with the resonant MOEMS EC-QCL. Here mode-hop free tuning was achieved by careful longitudinal mode control, i.e. by adjusting the external resonator length in combination with a current tuning. To adjust the resonator length, the MOEMS scanner was installed on a linear piezo-driven stage. Similar to the quasistatic MOEMS, the resonant MOEMS scanner plate has a circular shape 5 mm in diameter, into which again a grating is etched into.⁴ Here we use a grating with 190 l/mm.

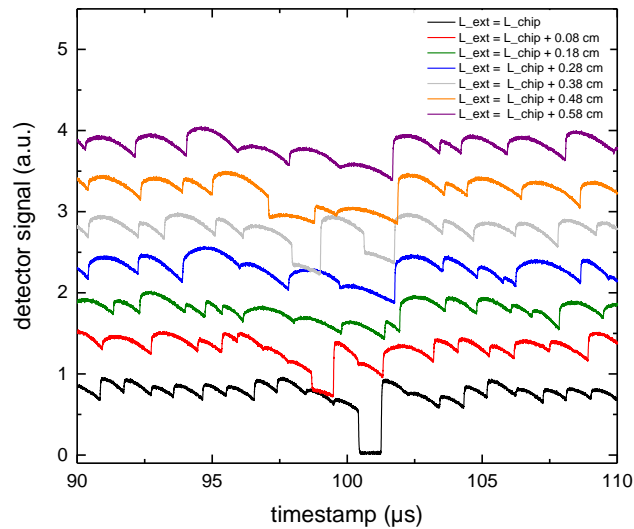


Figure 6. Intensity vs. time (\rightarrow grating angle) during a MOEMS scan for various length settings of the external resonator, demonstrating regular (black line) behavior with steps of identical length, as well as hardly predictable situations (e.g. green line). Note that the “dip” in intensity at $\sim 101 \mu\text{s}$ is due to atmospheric water absorption between laser and detector and not a feature of the laser itself.

This module allows us to investigate the influence of the total resonator length in relation to the optical length of the chip on the mode-hop behavior during a MOEMS scan, i.e. 1 ms. The QCL was operated in CW and was able to emit in the range of 1330 to 1450 cm^{-1} . The intensity as a function of the time, i.e. grating angle, after the provided MOEMS synchronization signal for different ratios between internal and external resonator are shown in Figure 6. For optimized length values, we observe a regular and stable mode pattern. Without this optimization, a hardly predictable sequence of mode hops with different spectral width and, at some wavelengths, reduced reproducibility may emerge, especially at unfortunate internal to external length combinations. For a given resonator length, only a set of discrete wavelengths is allowed. The wavelength is constant in between mode-hops and changes abruptly at a mode-hop. At the same time, the laser intensity changes. The discontinuities in the intensity signal in Fig. 6 corresponds therefore to a spectral mode-hop. This mode hop structure limits the spectral resolution that can be achieved.

To increase the spectral resolution, different length and current settings for each wavelength are required.⁸ The linear stage used in our setup is not fast enough to track the MEMS motion directly and the dynamic range for the laser current is far too small to cover the entire tuning range, i.e. adaptations cannot be made during a single full scan over e.g. $\sim 100 \text{ cm}^{-1}$. However, high resolution can be obtained by combining several subsequent scans, each containing a stable mode hop pattern, with varying length and current. The results of such a simultaneous variation is shown in Fig. 7. The mode

hop pattern, and therefore also the real emission wavelengths are shifted slightly between each variation in a very controlled manner. By combining several subsequent scans, the resolution can be increased. Under the given conditions, the mode-hop spectral distance is $\sim 0.4 \text{ cm}^{-1}$. Therefore, combining e.g. 20 scans can provide a resolution of $0.4/20 \text{ cm}^{-1} = 0.02 \text{ cm}^{-1}$, suitable for gas spectroscopy at atmospheric pressure. Increasing the number of scans can further reduce this resolution, ultimately limited by the linewidth of the cw-QCL over the resulting measurement time.

A demonstration of this approach is shown in Figure 8 for which 400 individual scans were recorded, and the resulting trace of the combined spectra was averaged in spectral direction over 10 spectra, leading to a final spectrum with 0.01 cm^{-1} resolution.

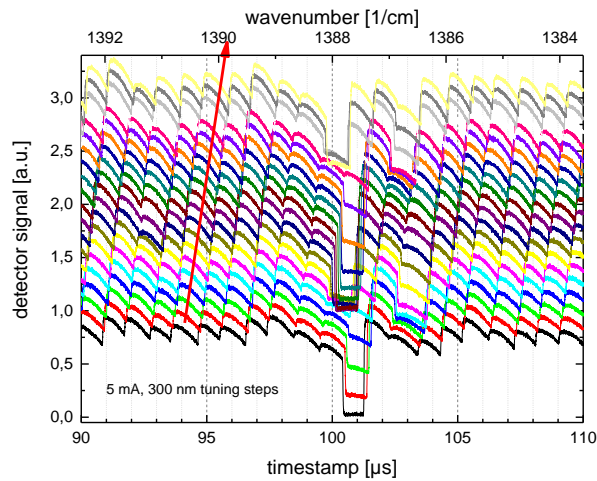


Figure 7. Principle of high spectral resolution by combining several scans with different length / current settings. The wavelength is constant in between mode hops ($\sim 1 \mu\text{s}$ in this example) and shifted slightly in every new trace by length / current adaption.

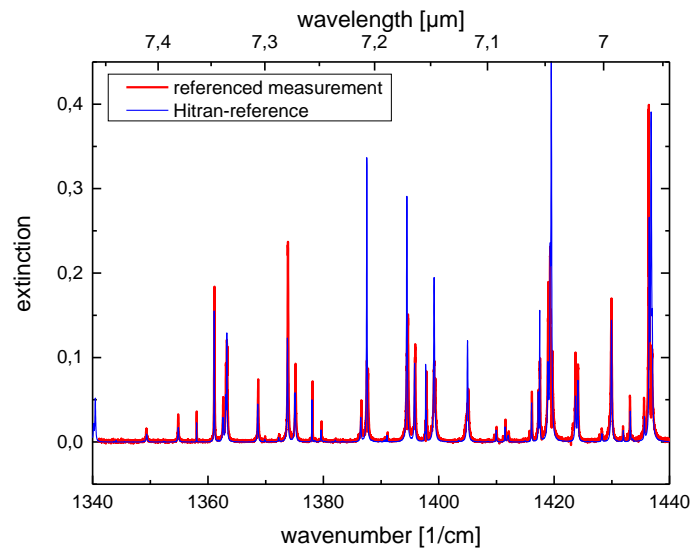


Figure 8. Demonstration of a high-resolution transmission spectrum of water vapor obtained with a fast-scanning MOEMS EC-QCL on a linear positioner.

In our proof-of-principle demonstration the mere acquisition time was indeed only 400 ms for 400 spectra. However, due to the communication overload with the data acquisition system, the laser current source, and the piezo stage the whole process currently still takes many seconds for a full scan containing 400 single spectra in this example. Currently we work on MOEMS diffraction grating with additional length control and on a high-speed FPGA-based data acquisition system, that would allow to truly exploit the high measurement speed enabled by the kHz-Scan rate of the current MOEMS device.

4. CONCLUSIONS

We presented recent results on a quasistatic MOEMS EC-QCL that is capable to tune to selected wavelength or to perform arbitrary angle trajectory movements. The laser module itself is matchbox-sized. This compact laser source is ideal for applications with large time constants as common for photothermal or photoacoustic spectroscopy. The small footprint is ideal to develop novel extremely compact devices, that bring IR spectroscopy from the lab to the field.

We also presented results on high resolution spectroscopy with a resonantly driven MOEMS EC-QCL, that performs wavelength scans at a rate of 1kHz. By careful mode control, i.e. cavity length and current tuning, high resolution spectra have been constructed. We have demonstrated that high-resolution spectroscopy with such a system is not only possible over a few wavenumbers,⁸ but over the whole tuning range of the QCL chip of more than 100 wavenumbers. This system has the potential for real-time high resolution spectroscopy over more than hundred of wavenumbers in a very compact footprint.

5. ACKNOWLEDGEMENTS

Part of the research leading to these results has received funding from the European Community's Horizon 2020 program under Grant Agreements 731465 AQUARIUS and 688265 MIRPHAB.

REFERENCES

- [1] Zhou, W., Bandyopadhyay, N., Wu, D., McClintock, R. and Razeghi, M., "Monolithically, widely tunable quantum cascade lasers based on a heterogeneous active region design," *Scientific Reports* 6, 25213 (2016).
- [2] Phillips, M.C., Taubman, M.S., Bernacki, B.E., Cannon, B.D., Schiffern, J.T. and Myers, T.L., "Design and performance of a sensor system for detection of multiple chemicals using an external cavity quantum cascade laser," *Proc. SPIE* 7608, 76080D (2010).
- [3] Grahmann, J., Merten, A., Ostendorf, R., Fontenot, M., Bleh, D., Schenk, H. and Wagner, H.-J., "Tunable External Cavity Quantum Cascade Lasers (EC-QCL) an Application Field for MOEMS Based Scanning Gratings," *Proc. of SPIE* Vol. 8977, 897708 (2014).
- [4] Grahmann, J., Merten, A., Herrmann, A., Ostendorf, R., Bleh, D., Drabe, C. and Kamenz, J., "Large MOEMS diffraction grating results providing an EC-QCL wavelength scan of 20 %," *Proc. SPIE* 9375, 93750W (2015).
- [5] Wagner, J., Ostendorf, R., Grahmann, J., Merten, A., Hugger, S., Jarvis, J.-P., Fuchs, F., Boskovic, D. and Schenk, H., "Widely tunable quantum cascade lasers for spectroscopic sensing," *Proc. SPIE* 9370, 937012 (2015).
- [6] Ostendorf, R., Butschek, L., Hugger, S., Fuchs, F., Yang, Q., Jarvis, J., Schilling, C., Rattunde, M., Merten, A., Grahmann, J., Boskovic, D., Tybussek, T., Rieblinger, K. and Wagner, J., "Recent Advances and Applications of External Cavity-QCLs towards Hyperspectral Imaging for Standoff Detection and Real-Time Spectroscopic Sensing of Chemicals," *Photonics* 3, 28 (2016).
- [7] Butschek, L., Hugger, S., Jarvis, J., Haertelt, M., Merten, A., Schwarzenberg, M., Grahmann, J., Stothard, D.M., Warden, M., Carson, C., Macarthur, J., Fuchs, F., Ostendorf, R. and Wagner, J., "Micro-opto-electromechanical systems-based external cavity quantum cascade lasers for real-time spectroscopy," *Optical Engineering*, 57(1), 011010 (2017).

- [8] Wysocki, G., Curl, R.F., Tittel, F.K., Maulini, R., Bulliard, J.M. and Faist, J., "Widely tunable mode-hop free external cavity quantum cascade laser for high resolution spectroscopic applications," *Appl. Phys. B* 81, 769-777 (2005).
- [9] Caffey, D., Radunsky, M.B., Cook, V., Weida, M. Buerki, P.R., Crivello, S. and Day, T., "Recent Results from Broadly Tunable External Cavity Quantum Cascade Lasers," *Proc. Of SPIE Vol. 7953* 79531K
- [10] Sandner, T., Graßhoff, T., Schwarzenberg, M., Schroedter, R. and Schenk, H., "Quasistatic microscanner with linearized scanning for an adaptive three-dimensional laser camera," *Journal of Micro/Nanolithography, MEMS, and MOEMS* 13 (1), 011114-1 - 011114-10 (2014).
- [11] Merten, A., Schroedter, R., Dreyhaupt, A., Graßhoff, T., Schwarzenberg, M., Hugger, S., Schilling, C., Grahmann, J., Ostendorf R., "Quasi-statischer MOEMS-Gitterscanner zum spektralen Durchstimmen eines MIR Quantenkaskadenlasers" accepted by *tm-technisches Messen de-Gruyter* at 2019/1/27
- [12] Schroedter, R., Schwarzenberg, M., Dreyhaupt, A., Barth, R., Sandner, T., Janschek, K., "Microcontroller based closed-loop control of a 2D quasi-static/resonant microscanner with on-chip piezo-resistive sensor feedback", *Proc. SPIE OPTO, MOEMS and Miniaturized Systems XVI*, 1011605, 2017, San Francisco, DOI: 10.1117/12.2251802